Nanoliposomes Containing Iodine and ZIF-8 Conjugated with Anti-CD20 Antibody: One Nanoplatform for Treatment and Imaging

Sajedeh Mahmoudzadeh , Negar Motakef Kazemi , Ali Jebali *

Posted Date: 7 May 2025

doi: 10.20944/preprints202505.0362.v1

Keywords: Nanoliposomes; Iodine; ZIF-8; Anti-CD20 counter acting agent; Poisonous quality; Anti-inflammatory properties

 doi:10.20944/preprints202505.0362.v1

Article

Nanoliposomes Containing Iodine and ZIF-8 Conjugated with Anti-CD20 Antibody: One Nanoplatform for Treatment and Imaging

Sajedeh Mahmoudzadeh [1,2], Negar Motakef Kazemi [2,3] and Ali Jebali [2,3,*]

[1] Medical Genomics Research Center, Tehran Medical Sciences Islamic Azad University, Tehran, Iran
[2] Department of Medical Nanotechnology, Faculty of Advanced Sciences and Technology, Tehran Medical Science, Islamic Azad University, Tehran, Iran
[3] Department of Nanobiomimetic, Faculty of Advanced Sciences and Technology, Tehran Medical Sciences, Islamic Azad University, Tehran, Iran
* Correspondence: alijebal2011@gmail.com

Abstract: Multifunctional nanoparticles have made used for the concurrent determination and treatment of intense and incessant fiery maladies. Our aim was to plan, synthesize and characterize nano-liposomes containing iodine and ZIF-8 conjugated with anti-CD20 antibody and to examine its differentiate property against X-rays. Their biocompatibility and anti-inflammatory properties of this nanoplatform was investigated invitro. In this study, the synthesis and characterization of nano-liposomes containing iodine and ZIF-8 conjugated with anti-CD20 antibody were performed using methods such as TEM, SEM, FTIR and DLS. The HU (Hansfeld) number of the synthesized nano-liposomes was determined using CTscan. Then, the cell death of white blood cells after exposure to synthesized nanoliposomes was measured by MTT test. Also, the anti-inflammatory properties of synthesized nanoliposomes were evaluated by ELISA kit measuring the amount of interferon gamma. Microscopic imaging with TEM and SEM and analysis with DLS showed that nanoliposomes containing iodine and ZIF-8 and conjugated with anti-CD20 antibody were spherical and had a size range of 150 to 300 nm. The binding of antibody on the surface of nanoliposomes was also confirmed in FTIR test. This study showed that the percentage of iodine loading was 76% and ZIF8 was 72% in synthesized nanoliposomes. Also, the percentage of antibody conjugation on synthesized nanoliposomes was reported to be 86%. Imaging with a CTscan device also showed that there was no significant difference between the Hounsfield number of different nanoliposomes. Also, the concentration dependence was not observed. MTT test also showed that among the different substances tested, iodine and ZIF8 nanoparticles had significant toxicity compared to the other substances tested at all concentrations. This shows that nanoliposomization of iodine and ZIF8 reduced toxicity on white blood cells. Also, ELISA test and determination of the amount of interferon gamma secretion clearly showed that anti-CD20 antibody and nanoliposomes containing this antibody were able to significantly reduce interferon gamma secretion by human white blood cells at all concentrations studied.

Keywords: nanoliposomes; iodine; ZIF-8; Anti-CD20 counter acting agent; poisonous quality; anti-inflammatory properties

Introduction

CD20 is a non-glycosylated phosphoprotein of 33-37 kDa that is expressed on the surface of almost all normal and malignant B cells [1]. It is also the target of rituximab, the most effective anticancer monoclonal antibody developed to date. Rituximab has already been prescribed to more than 300,000 lymphoma patients in the past decade and, interestingly, is now being investigated for use in other disorders such as autoimmune conditions including rheumatoid arthritis (RA) and

 doi:10.20944/preprints202505.0362.v1

systemic lupus erythematosus. Despite its success in immunotherapy, information on the biology of CD20 is still relatively scarce, in part because it has no known natural ligand and CD20 knockout mice have a nearly normal phenotype. However, interesting information has emerged from the work, suggesting that CD20 resides in lipid raft domains of the plasma membrane, where it likely functions as a storage calcium channel after binding to the B cell receptor for antigen in the present review. These and data on its activity as a therapeutic target will be discussed in depth in the present review. It is clear that a greater understanding of the biology of CD20, the mechanisms involved such as antibody-dependent cytotoxicity, complement cytotoxicity and the growth conditions that interact with anti-CD20 antibodies in vivo, will allow for the effective exploitation of CD20 as a therapeutic target [1–3].

CD20, or B-lymphocyte antigen, is expressed on all B-cell surfaces, starting from the pro-B phase (CD45R+, CD117+) and gradually increasing in concentration until maturity. In humans, CD20 is encoded by the MS4A1 gene. This gene encodes a member of the membrane-spanning4A family. Members of this novel protein family are characterized by shared structural features and similar intron/exon junction boundaries and show unique expression patterns among hematopoietic cells and non-lymphoid tissues. This gene encodes a B-lymphocyte surface molecule that is involved in the development and differentiation of B cells into plasma cells. This family member is located among a group of family members at 11q12. Alternative splicing of the human MS4A1 gene results in at least three transcripts (1 to 3) encoding the same protein. Variants 1 and 2 are poorly translated due to upstream open reading frame inhibition and stem-loop structures in their 5' untranslated regions. The relative abundance of the translatable version 3 versus poorly translated variants 1 and 2 may be a key determinant of CD20 levels in normal and malignant human B-cells and their responses to CD20-directed immunotherapies [4,5].

Imaging of the immune system and inflammatory response provides information about disease progression and severity to the extent possible. Of course, given that clinical imaging such as CT and MRI typically contain anatomical information, the presence or absence of an inflammatory state must be inferred from structural abnormalities; however, improvements in available contrast agents have made it possible to obtain functional as well as anatomical information. Improved in vivo imaging of inflammation will facilitate not only diagnosis but also patient monitoring for better care. Nowadays, imaging systems that provide limited anatomical and physiological information are widely used clinically, such as computed tomography (CT), magnetic resonance imaging (MRI), and ultrasound (US). [2] Monocytes and macrophages phagocytose pathogens by uptake at the site of infection, and in this way exogenous imaging agents can also be internalized and the inflammatory response can be imaged. Molecular imaging of these cells, of course, allows for noninvasive and in vivo visualization of these cells to determine the extent and severity of the disease. The visualization of immune cells as inflammatory biomarkers has great implications for the fields of personalized medicine and early diagnosis of inflammatory diseases. Imaging of lymphocytes is mainly performed by radiolabeled antibodies [4–7]. Molecular imaging relies on the presence of endogenous or exogenous contrast agents to identify inflamed tissue. Relying on endogenous contrast is desirable because of the reduced risk to patients, and as a result, molecular imaging typically requires tracer molecules specific to biological processes [8,9]. These tracers consist of a contrast agent, such as a fluorescent dye, that is targeted to a molecule/function within the body, providing high, controllable, and specific contrast versus endogenous contrast. Examples of tracers include radioactive atoms used in sugars to track metabolism with SPECT/PET [10], iodine-labeled tracers for X-ray-based imaging [11], and lanthanides that respond to an external magnetic field (MRI) [12]. However, further development of small molecule tracers has been significantly hampered by concerns about toxicity and poor sensitivity resulting from poor signal specificity and rapid clearance from the body. The use of nanoparticles is a potentially viable method for adding exogenous contrast for molecular imaging.

Our aim was to plan, synthesize and characterize nano-liposomes containing iodine and ZIF-8 conjugated with anti-CD20 antibody and to examine its differentiate property against X-rays

 doi:10.20944/preprints202505.0362.v1

Material and Methods

In this ponder, to begin with, the union and characterization of nanoliposomes containing iodine and ZIF-8 conjugated with anti-CD20 counter acting agent were performed. To synthesize ZIF-8 nanoparticles, zinc nitrate hexahydrate and 2-methylimidazole were blended and after mixing for 80 minutes, the arrangement was centrifuged at 10,000 rpm for 10 minutes to isolated ZIF-8 nanoparticles. After that, a arrangement of 100 mg/ml of potassium iodide and ZIF-8 was arranged in refined water. One ml of the extraordinary nanoliposome amalgamation unit with a concentration of 100 mg/ml was blended with one ml of potassium iodide and ZIF-8 arrangement and one ml of carboxy-PEG arrangement, and blended energetically for 5 minutes. At that point the gotten blend was centrifuged at tall speed of 10000 rpm and the supernatant was disposed of. Anti-CD20 counter acting agent was included to the accelerated arrangement and EDC buffer was included and blended enthusiastically once more for 5 minutes. After washing with physiological serum, the ultimate suspension was brought to a volume of 5 ml and characterized. Gas chromatography was utilized to guarantee the stacking of potassium iodide and ZIF8, and FTIR was utilized to demonstrate counter acting agent conjugation. Too, the measure run of nanoliposomes was assessed utilizing DLS and their shape and estimate were evaluated using TEM microscopy. Within the another step, the HU (Hansfeld) number of synthesized nanoliposomes was decided utilizing CTscan. Concentrations of 10, 5, 2, 1, and 0.5 mg/ml of the studied materials were arranged in a 96-well microplate, and after that it was imaged evenly and vertically employing a CTscan gadget and the Hounsfield number was measured utilizing computer program. Moreover, the poisonous quality of white blood cells was decided after presentation to the synthesized nanoliposomes. In this portion, to begin with 5 ml of blood was taken from a solid individual, matured 20 to 30 a long time, with no history of hereditary, irresistible, neurological, provocative, etc. illnesses, with educated assent, and after that white blood cells were isolated utilizing the Ficoll strategy and a cell suspension was made in RPMI1640 culture medium enhanced with 10% FBS at a thickness of 100,000 cells/ml. At that point, concentrations of 10, 5, 2, 1, and 0.5 mg/ml were arranged from distinctive bunches, and cell suspension was included to them and incubated for 24 hours at 37 degrees. After hatching, the reasonability was calculated utilizing the MTT strategy compared to the control. Within the final step, the anti-inflammatory properties of the synthesized nanoliposomes were decided. In this portion, additionally to the over step, white blood cells of a solid individual were separated utilizing the Ficoll strategy and a cell suspension was made in RPMI1640 culture medium improved with 10% FBS at a thickness of one hundred thousand cells/ml. At that point, 100 Î¼l of diverse bunches were arranged at concentrations of 10, 5, 2, 1, and 0.5 mg/ml, and 100 Î¼l of enacted white blood cell suspension was included and brooded for 24 hours at 37 degrees. After brooding, the cell supernatant was inspected and the intergalactic gamma concentration after presentation was decided utilizing an ELISA pack.

Results

SEM, TEM, and DLS: Figure 1 shows an image of nanoliposomes containing iodine and ZIF-8 and conjugated with anti-CD20 antibody using a TEM microscope. **Figure 1** also shows an image of ZIF8 nanoparticles using a SEM microscope. As can be seen in these two figures, the synthesized nanoliposomes are spherical and ZIF8 are hexagonal and separate. The size range of nanoliposomes containing iodine and ZIF-8 and conjugated with anti-CD20 antibody using DLS. The size range was 150 to 300 nm, the average size was 210 nm, the polydispersity index was 0.2 and the average positive zeta potential was 30 mV. Also, Figure 4-4- shows the size range of ZIF8 nanoparticles using DLS. The size range was 130 to 250 nm, the average size was 190 nm, the polydispersity index was 0.2 and the average positive zeta potential was 10 mV. As is clear, with nanoliposomalization, the size increased and the surface charge also increased.

 doi:10.20944/preprints202505.0362.v1

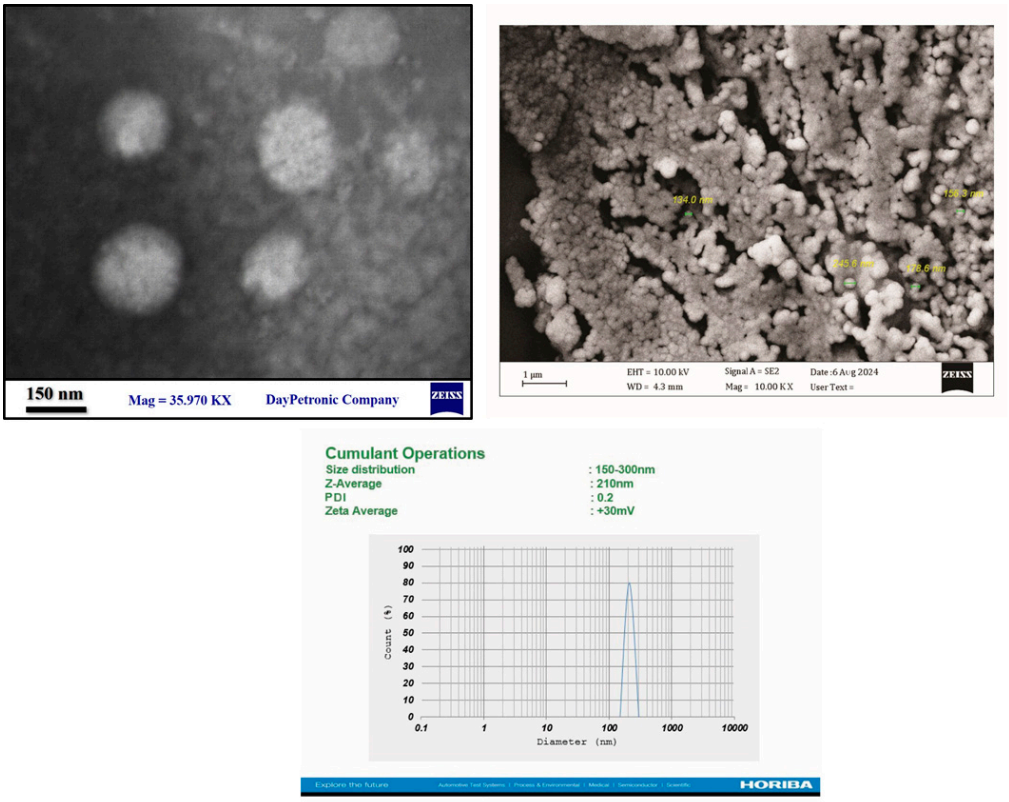

Figure 1. The TEM (left), SEM (right), and DLS (down) of nanoliposomes containing iodine and ZIF-8 and conjugated with anti-CD20 antibody.

FTIR: In the FTIR test, it was also determined that the absorption peaks of ZIF8 were at wave numbers 1102, 1236, and 1583, the absorption peaks of potassium iodide were at wave number 750, the absorption peaks of anti-CD20 antibody were at wave numbers 11800-1600 cm-1, 11570-1470 cm-1, and 11350-1250 cm-1, and the absorption peaks of nanoliposomes without antibody were at cm-1 801, cm-1 1355, cm-1 1740, cm-1 2852, and cm-1 2943. Also, the absorption peaks of nanoliposomes containing antibody were at wave numbers of 1800-1600 cm-1, 1570-1470 cm-1, 1350-1250 cm-1, 801 cm-1, 1355 cm-1, 1740 cm-1, and 2852 cm-1, which were the sum of the absorption peaks of antibody and nanoliposomes, indicating the binding of antibody on the nanoparticle surface.

Loading: According to Table 2, the percentage of iodine loading was 76% and ZIF-8 was 72% in the synthesized nanoliposomes. Also, the percentage of antibody conjugation on the synthesized nanoliposomes was reported to be 86%.

Biological tests

Based on **Figure 2,** there was no significant difference between the Hounsfield number of different nanoliposomes. Also, the dependence on concentration was not so visible. Considering that the Hounsfield number of water is zero and bone is about 2000, it can be indirectly judged that nanoliposomes synthesized with a Hounsfield number of about 500 can be used for imaging inflammatory areas. The Hounsfield number of all substances studied (NP1, NP2, NP3, NP4, NP5, NP6, NP7, NP8, ZIF8, iodine, and anti-CD20 antibody) had a significant difference with iodine at concentrations of 10, 5, and 2 mg/ml ($P<0.05$). Figure 4b shows the serial toxicity of different concentrations of NP1, NP2, NP3, NP4, NP5, NP6, NP7, NP8, ZIF8, iodine and anti-CD20 antibody on human white blood cells. Among the different substances tested, iodine and ZIF8 nanoparticles at all concentrations had significant toxicity compared to the other tested substances including NP1, NP2, NP3, NP4, NP5, NP6, NP7, NP8 and anti-CD20 antibody. This indicates that nanoliposomization of iodine and ZIF8 caused a significant (4-fold reduction) reduction in toxicity on white blood cells ($P<0.05$). Figure 2c Serial effect of NP1, NP2, NP3, NP4, NP5, NP6, NP7, NP8,

 doi:10.20944/preprints202505.0362.v1

ZIF8, iodine and anti-CD20 antibody on the secretion of interferon gamma by human white blood cells. It is clearly evident that anti-CD20 antibody and nanoliposomes containing this antibody were able to significantly reduce the secretion of interferon gamma by human white blood cells at all concentrations studied. The greatest decrease in interferon concentration (4-fold decrease) was seen at a concentration of 10 mg/ml NP1, NP 5, NP7, NP8.

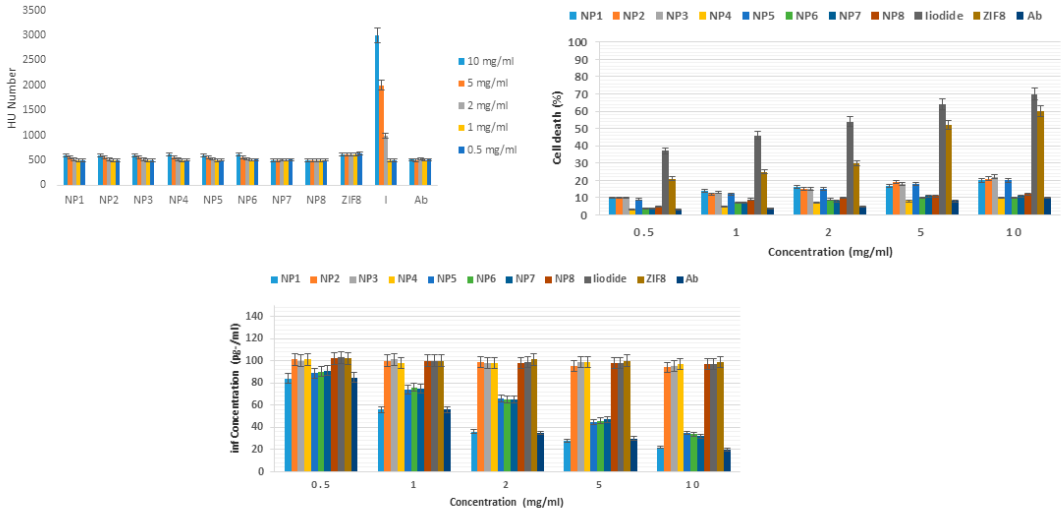

Figure 2. Hounsfield number (left), toxicity (right), and anti-inflammatory property (down) of NP1-NP8.

NP1: Nanoliposomes containing iodine and ZIF-8 and conjugated with anti-CD20 antibody
NP2: Nanoliposomes containing iodine and ZIF8 without anti-CD20 antibody
NP3: Nanoliposomes containing iodine but without anti-CD20 antibody
NP4: Nanoliposomes containing ZIF8 without anti-CD20 antibody
NP5: Nanoliposomes containing iodine with anti-CD20 antibody
NP6: Nanoliposomes containing ZIF8 with anti-CD20 antibody
NP7: Nanoliposomes without iodine and ZIF8 but with anti-CD20 antibody
NP8: Nanoliposomes without iodine and ZIF8 and anti-CD20 antibody
ZIF8: ZIF8
I: Iodine
Ab: Anti-CD20 antibody

Discussion

The point of this consider was to plan, synthesize and characterize nanoliposomes containing iodine and ZIF-8 conjugated with anti-CD20 counter acting agent and to explore their X-ray differentiate properties, assess their biocompatibility and anti-inflammatory properties in vitro for the treatment and imaging of fiery regions. Minuscule imaging and DLS test of nanoliposomes containing iodine and ZIF-8 and conjugated with anti-CD20 counter acting agent appeared that these structures were circular with a estimate extend of 150 to 300 nm, an normal measure of 210 nm, a polydispersity file of 0.2 and an normal positive zeta potential of 30 mV. The authoritative of counter acting agent on the surface of nanoliposomes was moreover affirmed in FTIR test. This consider appeared that the rate of iodine stacking was 76% and ZIF8 was 72% within the synthesized nanoliposomes. Moreover, the rate of counter acting agent conjugation (official) on the synthesized nanoliposomes was detailed to be 86%. Imaging of microtubes containing distinctive concentrations of NP1, NP2, NP3, NP4, NP5, NP6, NP7, NP8, ZIF8, iodine and anti-CD20 counter acting agent with a CTscan gadget appeared that there was no noteworthy distinction between the Hounsfield number of distinctive nanoliposomes. Too, the reliance on concentration was not so obvious. Of course, considering that the Hounsfield number of water is zero and bone is almost 2000, it can be in a roundabout way judged that the synthesized nanoliposomes with a Hounsfield number of

 doi:10.20944/preprints202505.0362.v1

around 500 can be utilized for imaging fiery regions. Serial harmfulness think about of distinctive concentrations of NP1, NP2, NP3, NP4, NP5, NP6, NP7, NP8, ZIF8, iodine and anti-CD20 counter acting agent on human white blood cells moreover appeared that among the distinctive substances tried, iodine and ZIF8 nanoparticles at all concentrations had critical harmfulness compared to other substances tried counting NP1, NP2, NP3, NP4, NP5, NP6, NP7, NP8 and anti-CD20 counter acting agent. This demonstrates that nanoliposomization of iodine and ZIF8 diminished harmfulness on white blood cells. Too, ELISA test and assurance of the sum of intergalactic gamma emission clearly appeared that anti-CD20 counter acting agent and nanoliposomes containing this counter acting agent at all concentrations tried were able to essentially decrease intergalactic gamma discharge by human white blood cells. This ponder is being conducted for the primary time and no comparative consider was found on the web. A few related considers are given here. In a ponder titled â CD20 antigen imaging with 124I-rituximab PET/CT in patients with rheumatoid arthritisâ by L Tran et al. in 2011, it was claimed that CD20 antigen expression may be a apparatus to localize destinations of irritation and have tall esteem within the determination and ensuing treatment of patients with rheumatoid joint pain. Here, an anti-CD20 monoclonal counter acting agent, rituximab (Mabthera) with 124I was appeared to be viable, and they detailed the primary 124I-rituximab PET/CT comes about in patients with rheumatoid joint pain [27]. In another consider, the impact of anti-CD20 treatments on gastrointestinal mucosal resistant homeostasis and their affiliation with fiery bowel infection in numerous sclerosis [28] was investigated. Another study examined the anti-CD20 counter acting agent rituximab within the treatment of rheumatoid joint pain and expressed that rheumatoid joint pain (RA) may be a unremitting systemic provocative infection based on immune reaction that influences joints and a few other organs. In spite of the fact that anti-TNF treatment and combination treatment with conventional anti-rheumatic drugs have demonstrated to treat RA, a noteworthy extent of patients still don't accomplish an satisfactory anti-rheumatic reaction. Rituximab, an anti-CD20 counter acting agent that depletes B cells, has been presented within the treatment of RA and has been appeared to be secure and successful in RA [29]. In another consider Anti-CD20 treatment in patients with rheumatoid joint pain: Indicator of reaction and B cell subset reconstitution after rehashed treatment by Petra Roll et al. in 2008, B cell exhaustion with the anti-CD20 counter acting agent, rituximab, in patients with RA and its adequacy have been demonstrated. The effects on B cell homeostasis after rehashed medications and the affiliation of certain B cell subsets with safe reactions or backslide are right now hazy (30). The short-term and long-term effects of anti-CD20 treatment on B cell ontogeny within the bone marrow of patients with rheumatoid joint pain were explored (31). In a survey by Marc D. Cohen, Edward Cornerstone in 2015, rituximab could be a chimeric monoclonal counter acting agent that targets the CD20 particle on the surface of a few but not all B cells. It depletes nearly all fringe B cells, but other B cell specialties (spaces, clefts) are dynamically drained, counting the synovium. Its component of activity in RA is as it were mostly caught on. Rituximab was successful in clinical trials of patients with RA, counting patients who had an inadequate reaction to methotrexate and those who had an fragmented reaction to tumor corruption factor inhibitors. Rot figure inhibitors require a concomitant conventional disease-modifying medicate, and the optimal dose of rituximab and the ideal interim for retreatment are to some degree vague. Rituximab shows up to be successful in seropositive patients and those who have an fragmented reaction to as it were one tumor corruption figure inhibitor. Rituximab contains a sensible security profile with a moo hazard of genuine irresistible occasions that's steady over time and with rehashed courses. Artful diseases are uncommon. Hepatitis B reactivation remains a concern. The conceivable affiliation ofrituximab and dynamic multifocal leukoencephalopathy may still require advance examination.

Conclusion

Imaging of microtubes containing distinctive concentrations of NP1, NP2, NP3, NP4, NP5, NP6, NP7, NP8, ZIF8, iodine and anti-CD20 counter acting agent with a CTscan appeared that there was no critical distinction between the Hounsfield number of distinctive nanoliposomes. Moreover, the reliance on concentration was not so obvious. Be that as it may, considering that the Hounsfield number of water is zero and bone is almost 2000, it can be by implication judged that nanoliposomes

 doi:10.20944/preprints202505.0362.v1

synthesized with a Hounsfield number of almost 500 can be utilized for imaging fiery zones. Serial concentrations of NP1, NP2, NP3, NP4, NP5, NP6, NP7, NP8, ZIF8, iodine, and anti-CD20 counter acting agent on human white blood cells too appeared that, among the diverse substances tried, iodine and ZIF8 nanoparticles at all concentrations had critical poisonous quality compared to other substances tried counting NP1, NP2, NP3, NP4, NP5, NP6, NP7, NP8, and anti-CD20 counter acting agent. This appeared that nanoliposomization of iodine and ZIF8 decreased poisonous quality on white blood cells. Too, ELISA test and assurance of the interfron gamma clearly appeared that anti-CD20 acting agent and nanoliposomes were able to altogether decrease inflammation.

References

1. Gao Y. Complement system in Anti-CD20 mAb therapy for cancer: A mini-review. International Journal of Immunopathology and Pharmacology. 2023;37(1):03946320231181464-9.
2. Kircher MF, Willmann JK. Molecular body imaging: MR imaging, CT, and US. part I. principles. Radiology. 2012;263(3):633-43.
3. Malviya G, Galli F, Sonni I, Signore A. Imaging T-lymphocytes in inflammatory diseases: a nuclear medicine approach. The Quarterly Journal of Nuclear Medicine and Molecular Imaging. 2014;58(3):237-57.
4. Malviya G, Anzola K, Podestà E, Laganà B, Del Mastro C, Dierckx R. 99m Tc-labeled rituximab for imaging B lymphocyte infiltration in inflammatory autoimmune disease patients. Molecular imaging and biology. 2012;14(2):637-46.
5. Moroz MA, Zhang H, Lee J, Moroz E, Zurita J, Shenker L. Comparative analysis of T cell imaging with human nuclear reporter genes. Journal of Nuclear Medicine. 2015;56(7):1055-60.
6. Tavaré R, McCracken MN, Zettlitz KA, Salazar FB, Olafsen T, Witte ON. Immuno-PET of murine T cell reconstitution postadoptive stem cell transplantation using anti-CD4 and anti-CD8 cys-diabodies. Journal of Nuclear Medicine. 2015;56(8):1258-64.
7. Zalev J, Richards LM, Clingman BA, Harris J, Cantu E, Menezes GL. Opto-acoustic imaging of relative blood oxygen saturation and total hemoglobin for breast cancer diagnosis. Journal of Biomedical Optics. 2019;24(12):121915-9.
8. Lee J, Hirano Y, Fukunaga M, Silva AC, Duyn JH. On the contribution of deoxy-hemoglobin to MRI gray–white matter phase contrast at high field. Neuroimage. 2010;49(1):193-8.
9. McGale J, Khurana S, Huang A, Roa T, Yeh R, Shirini D, Doshi P, Nakhla A, Bebawy M, Khalil D, Lotfalla A. PET/CT and SPECT/CT imaging of HER2-positive breast cancer. Journal of Clinical Medicine. 2023;12(15):4882-9.
10. Lee N, Choi SH, Hyeon T. Nano-sized CT contrast agents. Advanced Materials. 2013;25(19):2641-60.
11. Wang HL, Liu D, Jia JH, Liu JL, Ruan ZY, Deng W, Yang S, Wu SG, Tong ML. High-stability spherical lanthanide nanoclusters for magnetic resonance imaging. National Science Review. 2023;10(4):036-42.
12. Pearce AK, O'Reilly RK. Insights into active targeting of nanoparticles in drug delivery: advances in clinical studies and design considerations for cancer nanomedicine. Bioconjugate chemistry. 2019;30(9):2300-11.
13. Desar I, Van Herpen C, Van Laarhoven H, Barentsz J, Oyen W, Van Der Graaf W. Beyond RECIST: molecular and functional imaging techniques for evaluation of response to targeted therapy. Cancer treatment reviews. 2010;35(4):309-21.
14. Gallagher F. An introduction to functional and molecular imaging with MRI. Clinical radiology. 2010;65(7):557-66.
15. Caravan P. Strategies for increasing the sensitivity of gadolinium based MRI contrast agents. Chemical Society Reviews. 2016;35(6):512-23.

 doi:10.20944/preprints202505.0362.v1

16. Jin R, Lin B, Li D, Ai H. Superparamagnetic iron oxide nanoparticles for MR imaging and therapy: design considerations and clinical applications. Current opinion in pharmacology. 2014;18(1):18-27.
17. Wahajuddin n, Arora S. Superparamagnetic iron oxide nanoparticles: magnetic nanoplatforms as drug carriers. International journal of nanomedicine. 2012:1(1):3445-71.
18. Neuwelt A, Sidhu N, Hu C-AA, Mlady G, Eberhardt SC, Sillerud LO. Iron-based superparamagnetic nanoparticle contrast agents for MRI of infection and inflammation. AJR American journal of roentgenology. 2015;204(3):W302-8.
19. Manias KA, Peet A. What is MR spectroscopy? Archives of Disease in Childhood-Education and Practice. 2018;103(4):213-6.
20. Wu B, Warnock G, Zaiss M, Lin C, Chen M, Zhou Z. An overview of CEST MRI for non-MR physicists. EJNMMI physics. 2016;3(1):1-21.
21. Liu G, Bettegowda C, Qiao Y, Staedtke V, Chan KW, Bai R. Noninvasive imaging of infection after treatment with tumor-homing bacteria using Chemical Exchange Saturation Transfer(CEST)MRI. Magnetic resonance in medicine. 2013;70(6):1690-8.
22. Consolino L, Anemone A, Capozza M, Carella A, Irrera P, Corrado A. Non-invasive investigation of tumor metabolism and acidosis by MRI-CEST imaging. Frontiers in Oncology. 2020;10(1):161-8.
23. Chang L, Munsaka SM, Kraft-Terry S, Ernst T. Magnetic resonance spectroscopy to assess neuroinflammation and neuropathic pain. Journal of Neuroimmune Pharmacology. 2013;8(1):576-93.
24. Chen Y, Dai Z, Shen Z, Lin G, Zhuang C, Li H. Magnetic resonance imaging of glutamate in neuroinflammation. Radiology of Infectious Diseases. 2016;3(2):92-7.
25. Yanez Lopez M, Pardon M-C, Baiker K, Prior M, Yuchun D, Agostini A. Myoinositol CEST signal in animals with increased Iba-1 levels in response to an inflammatory challenge—Preliminary findings. PLoS One. 2019;14(2):e0212002-8.
26. Tarkin JM, Dweck MR, Evans NR, Takx RA, Brown AJ, Tawakol A. Imaging atherosclerosis. Circulation research. 2016;118(4):750-69.
27. Tran L, Huitema AD, van Rijswijk MH, Dinant HJ, Baars JW, Beijnen JH. CD20 antigen imaging with 124I-rituximab PET/CT in patients with rheumatoid arthritis. Human antibodies. 2011;20(1-2):29-35.
28. Quesada-Simó A, Garrido-Marín A, Nos P, Gil-Perotín S. Impact of Anti-CD20 therapies on the immune homeostasis of gastrointestinal mucosa and their relationship with de novo intestinal bowel disease in multiple sclerosis: a review. Frontiers in Pharmacology. 2023;14(2):1186016-20.
29. Korhonen R, Moilanen E. Anti-CD20 antibody rituximab in the treatment of rheumatoid arthritis. Basic & clinical pharmacology & toxicology. 2010;106(1):13-21.
30. Roll P, Dörner T, Tony HP. Anti-CD20 therapy in patients with rheumatoid arthritis: predictors of response and B cell subset regeneration after repeated treatment. Arthritis & Rheumatism: Official Journal of the American College of Rheumatology. 2008;58(6):1566-75.
31. Rehnberg M, Amu S, Tarkowski A, Bokarewa MI, Brisslert M. Short-and long-term effects of anti-CD20 treatment on B cell ontogeny in bone marrow of patients with rheumatoid arthritis. Arthritis research & therapy. 2009;11(1):1-12.
32. Cohen MD, Keystone E. Rituximab for rheumatoid arthritis. Rheumatology and therapy. 2015;2(1):99-111.